EAN 2019
57th conference on experimental stress analysis

Non-associated flow rule in the prediction of complex stress states and deformations

ŠEBEK František[1,a], KUBÍK Petr[1,b], PETRUŠKA Jindřich[1,c] and ZAPLETAL Josef[2,d]

[1]Institute of Solid Mechanics, Mechatronics and Biomechanics; Faculty of Mechanical Engineering; Brno University of Technology; Technická 2896/2, 616 69 Brno, Czech Republic

[2]Institute of Materials Science and Engineering; Faculty of Mechanical Engineering; Brno University of Technology; Technická 2896/2, 616 69 Brno, Czech Republic

[a]sebek@fme.vutbr.cz, [b]kubik.p@fme.vutbr.cz, [c]petruska@fme.vutbr.cz, [d]zapletal@fme.vutbr.cz

Keywords: Flow rule, Ductile fracture, Large plastic deformations, Lode parameter, Stress triaxiality

Abstract. The paper deals with the application of non-associated flow rule to the non-quadratic yield criterion. The utilization resulted in a significant improvement in the predicted stress states as well as deformations, which matched the theoretical values and experimental observations. The correct calibration of such an advanced plasticity model, and especially its plastic potential, will be subjected to a further research.

Introduction

The correct plasticity modelling is important when large plastic deformations occur. This may be found in many engineering applications [1–4]. The flow rule plays a vital role in the plasticity models. It determines the direction of the plastic strain increment. The flow rule might be either associated or non-associated. The associated one corresponds to equal yield function and plastic potential, which results in the plastic strain increment normal to the yield surface. The non-associated flow rule has a distinct yield function from the plastic potential, so that the plastic strain increment is not normal to the yield surface but to the plastic potential. It might seem as a minor model feature, but it can significantly influence the results [5]. It was shown that the force response can be improved by a non-quadratic plasticity model a lot [6, 7], but it significantly deteriorates the stress state [8–11] as well as the deformations [12].

Experiments

First, standard tensile tests were conducted on aluminium alloy 2024-T351 in order to estimate the elastic constants and flow curve. The flow curve estimation was based on the iterative procedure until the match between the simulation and experiment was satisfying. Then, upsetting tests of notched cylindrical specimens and tensile tests of flat grooved specimens were carried out in order to represent specific stress states [11] and complex deformations [12]. All the loadings in experiments were realized in the rolling direction of the supplied cold-rolled plate. In other words, the specimens' axes were parallel to this rolling direction.

Plasticity modelling

The experiments were modelled using three basic types of plasticity models. The first one was a classical von Mises yield criterion with associated flow rule having the equivalent stress as

$$\bar{\sigma} = \sqrt{\frac{1}{2}\left[\left(\sigma_1 - \sigma_2\right)^2 + \left(\sigma_2 - \sigma_3\right)^2 + \left(\sigma_3 - \sigma_1\right)^2\right]} \tag{1}$$

where $\sigma_1 \geq \sigma_2 \geq \sigma_3$ are the principal stresses ordered according to their magnitudes.

The second model had an associated flow rule as well, while the yield criterion was close to the Tresca one. This was utilized by a Hershey yield criterion [13] having the equivalent stress defined as

$$\bar{\sigma} = \sqrt[m]{\frac{1}{2}\left[\left|\sigma_1 - \sigma_2\right|^m + \left|\sigma_2 - \sigma_3\right|^m + \left|\sigma_3 - \sigma_1\right|^m\right]} \tag{2}$$

where m is the material constant, which was chosen equal to 100, so that it is close to the Tresca yield criterion. This model was implemented into Abaqus explicit finite element code using VUMAT user subroutine, as it is not available in that commercial software.

The last yield criterion was a Mohr–Coulomb one with non-associated flow rule, which is built in Abaqus. The yield function is [14]

$$f = R_{mc} q - p \tan\phi - c \tag{3}$$

where q is the von Mises equivalent stress according to the Eq. (1), p is the hydrostatic pressure, ϕ is the friction angle, c is the cohesion stress and R_{mc} is a function defined as [14]

$$R_{mc} = \frac{1}{\sqrt{3}\cos\phi}\sin\left(\Theta - \frac{\pi}{3}\right) + \frac{1}{3}\cos\left(\Theta - \frac{\pi}{3}\right)\tan\phi \tag{4}$$

where Θ is the Lode angle. This Lode angle can be normalized as

$$\bar{\Theta} = 1 - \frac{6}{\pi}\Theta \tag{5}$$

The friction angle was set to zero so that the yield criterion corresponded to Tresca one and was pressure independent. The cohesion stress was half the estimated flow stress with twice the equivalent plastic strain due to its formulation [14]

$$\bar{\varepsilon}_{pl} = \int \frac{1}{c}\boldsymbol{\sigma} : \mathrm{d}\varepsilon_{pl} \tag{6}$$

where $\boldsymbol{\sigma}$ is the Cauchy stress tensor and $\mathrm{d}\varepsilon_{pl}$ is the plastic strain increment. The plastic potential is a hyperbolic function in the meridional stress plane [14] and smooth elliptic function in the deviatoric stress plane, which was proposed by Menétrey and William [15]

$$g = \sqrt{\left(\varepsilon c_0 \tan\psi\right)^2 + \left(R_{mw} q\right)^2} - p\tan\psi \tag{7}$$

where ε is the meridional eccentricity defining the rate at which the hyperbolic function approaches the asymptote, c_0 is the initial cohesion stress, ψ is the dilation angle and R_{mw} function defined as [14]

$$R_{mw} = \frac{4\left(1-e^2\right)\cos^2\Theta + \left(2e-1\right)^2}{2\left(1-e^2\right)\cos\Theta + \left(2e-1\right)\sqrt{4\left(1-e^2\right)\cos^2\Theta + 5e^2 - 4e}} R_{mc}\left(\frac{\pi}{3}, \phi\right) \tag{8}$$

where e is the deviatoric eccentricity and $R_{mc}\left(\frac{\pi}{3}, \phi\right)$ from Eq. (4) simplifies into [14]

$$R_{mc}\left(\frac{\pi}{3}, \phi\right) = \frac{3-\sin\phi}{6\cos\phi} \tag{9}$$

Meridional eccentricity was set to 0.001 and the dilation angle to zero so the plastic potential was not pressure dependent, while the deviatoric eccentricity was defined as

$$e = \frac{3-\sin\phi}{3+\sin\phi} \tag{10}$$

The plastic potential has the shape according to the von Mises (a circle in a deviatoric plane).

Results and discussion

The results of computational simulations are compared to experiments in Fig. 1.

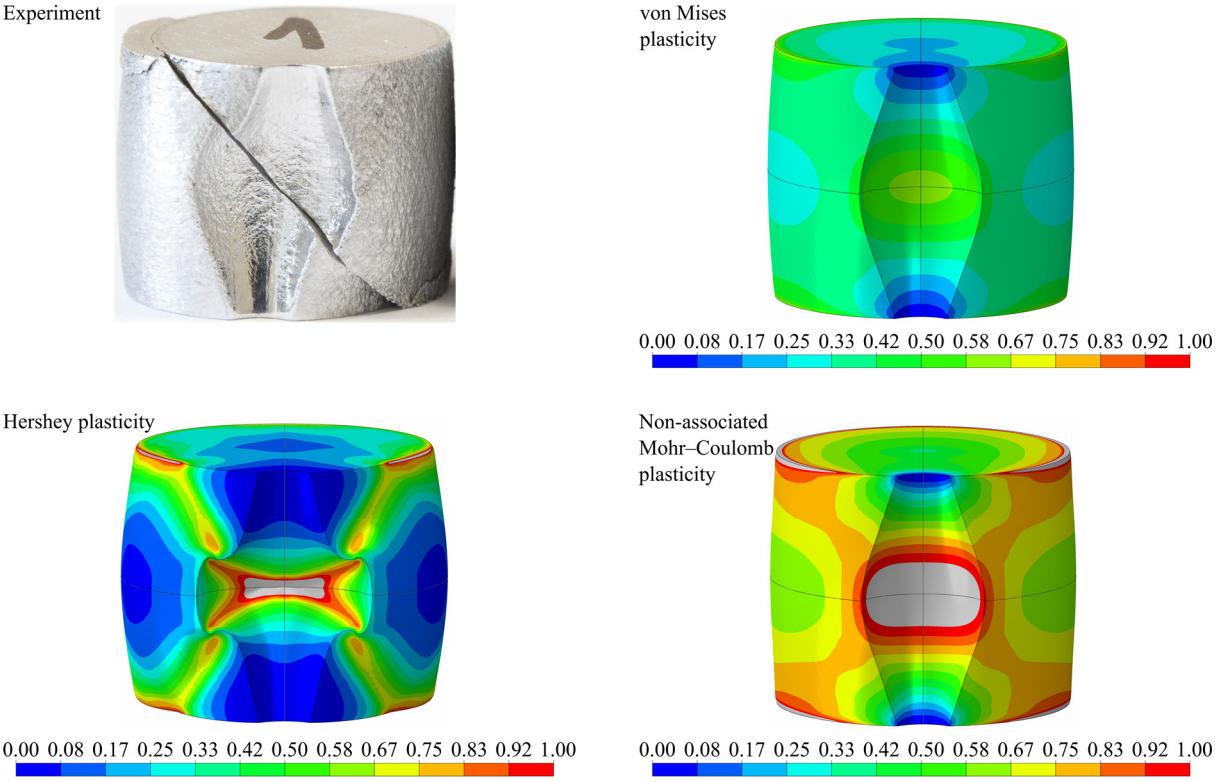

Fig. 1: Comparison of computational (equivalent plastic strain) and experimental results for the compression test

From Fig. 1, it is clear that the non-quadratic yield criterion according to Hershey (close to the Tresca one) predicted incorrectly the deformations. Remaining two plasticity models predicted the deformations in correspondence with experiment, but the Mohr–Coulomb yield criterion with non-associated flow rule resulted in significantly higher equivalent plastic strain.

Computationally obtained stress states for the tensile test of flat grooved specimen are in Fig. 2. Theoretically, the deviatoric stress state measure, normalized Lode angle from Eq. (5) in this case, should approach zero because the specimen underwent a generalized shear. The non-quadratic yield criterion (Hershey) improved the force response, but deteriorated the stress state, when compared to the quadratic one (Mises), both associated. The Mohr–Coulomb yield criterion with non-associated flow rule improved both the force response and stress state. But similar problem as in the case of upsetting test arose for this plasticity model, which predicted twice the equivalent plastic strain at fracture.

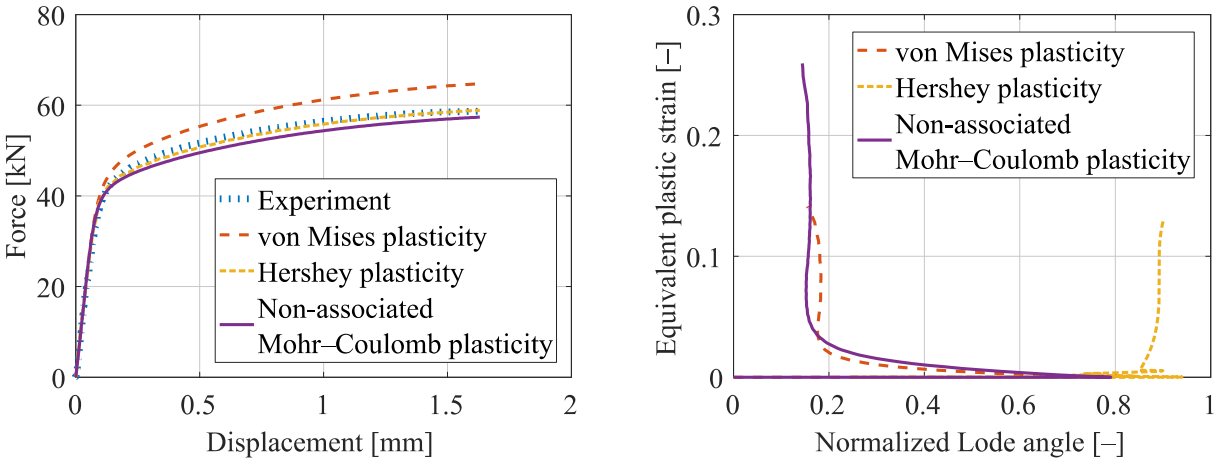

Fig. 2: Computational results for the tensile test of flat grooved specimen

This analysis is important, because correct stress state prediction is important especially for ductile fracture. It may be crucial for accurate simulation of the crack initiation and propagation [16, 17].

Conclusions

The non-associated flow rule has a significant role in the prediction of complex deformations. It has also a decisive role in the predicting of correct stress states, which are crucial in the ductile fracture simulations. This is going to be a hot topic for further research. Especially, the question of higher equivalent plastic strain for the non-associated flow rule when compared to the associated one has to be solved. It is also challenging to calibrate such an advanced plasticity model correctly.

Acknowledgement

This work was supported by the Czech Science Foundation under contract No. 19-20802S “A coupled real-time thermo-mechanical solidification model of steel for crack prediction.”

References

[1] F. Šebek, J. Hůlka, P. Kubík, J. Petruška, On the proportionality of damage rule in finite element simulations of the ductile failure, Adv. Mater. Res. 980 (2014) 189–193.

[2] J. Petruška, T. Návrat, F. Šebek, M. Benešovský, Optimal intermeshing of multi roller cross roll straightening machine, AIP Conference Proceedings 1769 (2016) 120002.

[3] M. Peč, P. Vosynek, F. Šebek, T. Návrat, Implementation of American weld connection standards into finite element computations, IOP Conference Series: Materials Science and Engineering 179 (2017) 012056.

[4] M. Španiel, T. Mareš, J. Kuželka, F. Šebek, J. Džugan, Uncoupled material model of ductile fracture with directional plasticity, In: Proceedings of the 14th International Conference on Computational Plasticity - Fundamentals and Applications, COMPLAS (2017) 596–605.

[5] X. Gao, T. Zhang, J. Zhou, S. M. Graham, M. Hayden, Ch. Roe, On stress-state dependent plasticity modeling: Significance of the hydrostatic stress, the third invariant of stress deviator and the non-associated flow rule, Int. J. Plast. 27 (2011) 217–231.

[6] F. Šebek, J. Petruška, P. Kubík, The performance and prediction ability of advanced approach to ductile fracture, In: Proceedings of the 14th International Conference on Computational Plasticity - Fundamentals and Applications, COMPLAS (2017) 588–595.

[7] F. Šebek, P. Kubík, J. Petruška, Application of coupled ductile fracture criterion to plane strain plates, Defect Diffus. Forum 382 (2018) 186–190.

[8] Y. Bai, T. Wierzbicki, A new model of metal plasticity and fracture with pressure and Lode dependence, Int. J. Plast. 24 (2008) 1071–1096.

[9] M. Kroon, J. Faleskog, Numerical implementation of a J_2- and J_3-dependent plasticity model based on a spectral decomposition of the stress deviator, Comput. Mech. 52 (2013) 1059–1070.

[10] M. Algarni, Y. Bai, Y. Choi, A study of Inconel 718 dependency on stress triaxiality and Lode angle in plastic deformation and ductile fracture, Eng. Fract. Mech. 147 (2015) 140–157.

[11] F. Šebek, J. Petruška, P. Kubík, Behavior of lode dependent plasticity at plane strain condition and its implication to ductile fracture, Solid State Phenom. 258 (2017) 213–216.

[12] P. Kubík, F. Šebek, J. Petruška, Notched specimen under compression for ductile failure criteria, Mech. Mater. 125 (2018) 94–109.

[13] A. V. Hershey, The plasticity of an isotropic aggregate of anisotropic face-centered cubic crystals. J. Appl. Mech. 53 (1954) 241–249.

[14] Abaqus. SIMULIA User Assistance 2017. Dassaul Systèmes Simulia Corporation, Providence, Rhode Island.

[15] P. Menétrey, K. J. William, Triaxial failure criterion for concrete and its generalization, ACI Struct. J. 92 (1995) 311–318.

[16] J. Petruška, P. Kubík, J. Hůlka, F. Šebek, Ductile fracture criteria in prediction of chevron cracks, Adv. Mater. Res. 716 (2013) 653–658.

[17] F. Šebek, P. Kubík, J. Petruška, Chevron crack prediction using the extremely low stress triaxiality test, MM Sci. J. (2015) 617–621.